

# UC Riverside

## UC Riverside Undergraduate Research Journal

### Title

Determination of Immune Signal–Receptors, PD-1 and PD-L1, Interactions in Solution using qFRET Technology

### Permalink

<https://escholarship.org/uc/item/2d09435x>

### Journal

UC Riverside Undergraduate Research Journal, 12(1)

### Authors

Nwangwu, Mary

Liao, Jiayu

### Publication Date

2018

### DOI

10.5070/RJ5121039167

### Copyright Information

Copyright 2018 by the author(s). This work is made available under the terms of a Creative Commons Attribution-NonCommercial License, available at

<https://creativecommons.org/licenses/by-nc/4.0/>

Peer reviewed

## Determination of Immune Signal–Receptors, PD-1 and PD-L1, Interactions in Solution using qFRET Technology

Mary Nwangwu<sup>1</sup>, Vipul Madahar<sup>1</sup>, Jiayu Liao<sup>1</sup>

<sup>1</sup> Department of Bioengineering

### ABSTRACT

Human PD-L1 (programmed cell death 1 - ligand 1) is a transmembrane protein that is highly expressed on the membrane of cancer cells. It binds to inhibitory receptor PD-1 (programmed cell death protein - 1), which is expressed on the surface of cytotoxic T cells. The interaction between PD-L1 and PD-1 reduces the effect of anti-tumor immune response and the strategy of blocking their interaction has been used for anti-cancer drug manufacture. Past studies isolated the extracellular domain of PD-L1 for characterization of the structure. This study aims to recover, isolate, and purify the insoluble PD-L1 protein (external domain), and study its binding interaction with PD-1 for the development of an *in vitro* quantitative FRET (qFRET) assay. To report PD-L1/PD-1 binding interaction, fluorescent donor and acceptor pairs, CyPet and YPet were bound to PD-L1 and PD-1 proteins respectively and qFRET was applied to assess the interaction of the two proteins based entirely on fluorescence.

The results provide evidence of recovery of the purified and refolded CyPet-Ext.PDL1 and YPet-Ext.PD1 proteins from cell pellets, shown in the coomassie stained SDS-PAGE gel. This study also shows that the proteins were able to be recovered through affinity chromatography under denaturing conditions. The qFRET technique showed that the acceptor, YPet-Ext.PD1, is interacting with the donor, CyPet-Ext.PDL1. This study provides a novel method for better understanding the binding mechanism of PD-L1/PD-1 that can be applied to other cell-surface protein interactions, as well as to stipulate a platform for small molecule inhibitor related drug screenings and production.

**Keywords:** PD-1, PD-L1, Expression, Immunotherapy, Antibody, FRET



### Mary Nwangwu

Department of Bioengineering

Mary Nwangwu is a fourth-year bioengineering major. She joined the Liao Lab in June 2017 and is presently working on protein renaturing and Förster resonance energy transfer-based high throughput screening assays. Mary's research on fluorescent tagged protein derivation from inclusion bodies is being funded by the Undergraduate Education Quarterly Minigrant. She is also currently working on a senior design project and intends to pursue a career in biotechnology.



### FACULTY MENTOR

#### Dr. Jiayu Liao

Associate Professor in the Department of Bioengineering

Professor Liao joined the University of California, Riverside as a founding faculty of the Bioengineering Department in 2006. At UCR, he has developed a novel quantitative FRET technology platform for biochemical parameter determinations and high-throughput screening assay for drug discovery. Professor Liao obtained his PhD from the School of Medicine at the University of California, Los Angeles. He attended the Scripps Research Institute for post-doctoral training, and subsequently joined the Genomic Institute of Novartis Research Foundation as Principal Investigator and Founding Scientist of GPCR platform before he joined UCR.

## INTRODUCTION

Cancer cells are characterized as cells that divide persistently and out of control. These abnormal cells form solid malignant tumors (abnormal body tissue growth) or flood the bloodstream. Cell division is a standard process in the body for tissue repair and growth. Healthy cells will divide until it is no longer necessary for them to do so, but cancerous cells continue to produce more copies of themselves. The classification of a cancer cell depends on the cell type from which it originates. These categories include, but are not limited to, Carcinoma (originating in membranous tissues that line the body), Sarcoma (originating in connective tissue such as muscle and bone), and Leukaemia (originating in tissues that produce new blood cells, mainly bone marrow).

Cancer immunotherapy involves the use of the immune system to treat cancer. The immune system consists of two parts: innate immunity and adaptive immunity. Innate immunity, or in built immune protection, is viewed as the defense an individual has from birth. The defenses rely heavily on barriers such as the skin, inner linings of organs, hair, inflammatory responses, and natural killer cells. Adaptive, or acquired, immunity is characterized as the protection developed after exposure to certain bacteria or diseases. The defenses include antibody production (B cells) and potentiating the function of accessory cells (natural killer cells, macrophages, etc.). Cell mediated response (T cells) is also a part of the adaptive immunity branch and is especially useful for fighting cancer cells. Different chemicals that can aid in the immune response can be produced *in vitro*. These different types of immunotherapy include monoclonal antibodies (mABs), vaccines, cytokines, and adoptive cell transfer.

Human PD-L1 (programmed cell death-ligand 1) is a transmembrane protein that is expressed on a wide variety of normal tissues, including natural killer cells, B cells, and endothelial cells.<sup>9</sup> It normally binds to inhibitory PD-1 (programmed cell death protein-1) receptors expressed on the surface of activated cytotoxic T cells. Cytotoxic T cells, or T lymphocytes, are central effectors to eliminate cancer cells in an antigen and cell contact dependent manner and induce long-lasting tumor regression.<sup>8</sup> PD-1/PD-L1 interaction inhibits T cell growth and the secretion

of cytokines, polypeptides that act on hematopoietic stem cells (cells that give rise to myeloid and lymphoid blood cells) and modulates immune and inflammatory responses. Hino et al. found that tumor cell-borne PD-L1 induces the apoptosis (programmed cell death) of tumor-specific T cell clones *in vitro*, suggesting the potential role of PD-L1 in tumor immunity.<sup>6</sup>

PD-L1 expression is heterogeneous across primary breast cancers and is generally associated with the presence of tumor-infiltrating lymphocytes and the presence of poor-prognosis features such as high grade, and aggressive molecular subtypes (triple-negative (TN), basal, HER2-enriched).<sup>2</sup> Clinical findings have shown that blockage of PD-1 and PD-L1 interaction by antibodies has a steadfast effect on many advanced tumors (*see Figure 1*). Monoclonal antibodies are a class of drugs called checkpoint inhibitors that hinder the interaction of PD-1 and PD-L1 and overcome the disadvantages of conventional anti-cancer therapy. *In vitro* and *in vivo* studies that were done by Lussier et al. showed that blocking PD-1 using an antibody can partially enhance T-cell function.<sup>1</sup>

Sales of the PD-1/PD-L1 therapy class have grown from \$84 million in 2014 to \$6,292 million in 2016, with five PD-1/PD-L1 inhibitors presently approved across a variety of tumor indications.<sup>5</sup> However, the developers of successful PD-1/PD-L1 based immunotherapies such as OPDIVO® and KEYTRUDA® still continue to face clinical and commercial challenges. As discussed by Meng et al., these challenges include the identification of optimal combinations, treatment-related adverse effects, the high cost and lack of effective predictive markers which make the aforementioned products less promising as widely used therapeutic options.<sup>11</sup> The utilization of qFRET to assess the small-scale binding mechanism of PD-1/PD-L1 can provide kinetic measurements that will give insight into what kind of effects these drugs will have overall. The overarching goal is to find a drug that will have optimal efficacy and minimal side effects.

The FRET (Förster resonance energy transfer) phenomenon is used to identify protein interactions, monitor intracellular signaling activities in real-time, and survey bioactive molecules by high-throughput screening.<sup>13</sup> It is a distance-

dependent physical process by which energy is transferred nonradiatively from an excited molecular fluorophore (the donor) to another fluorophore (the acceptor) by means of intermolecular long-range dipole-dipole coupling.<sup>12</sup> The excitation of the donor can elicit an energy transfer to induce emission from the acceptor when the two are close to each other (1-10 nm). This results in quenching of the donor and excitation of the acceptor. YPet (yellow fluorescent protein for energy transfer) is the acceptor fluorophore and CyPet (cyan fluorescent protein for energy transfer) is the donor fluorophore. Protein-protein interactions allow for CyPet and YPet to come into close range, permitting FRET to occur successfully. The quantitation of FRET can be made with a ratio metric determination of the two signals, as FRET results in both a decrease in fluorescence of the donor molecule as well as an increase in fluorescence of the acceptor.<sup>7</sup>

This study plans to recover, isolate, and purify both CyPet-Ext.PDL1 and YPet-Ext.PD-1 proteins. The efficiency of this procedure will be verified by SDS-PAGE (sodium dodecyl sulfate polyacrylamide gel electrophoresis). A fluorescence spectrum of CyPet-Ext.PDL1 and YPet-Ext.PD1 will be generated to confirm the presence of the fluorescent tags. The qFRET technique will then be applied to the two proteins and will provide evidence of binding interaction between PD-L1 and PD-1.

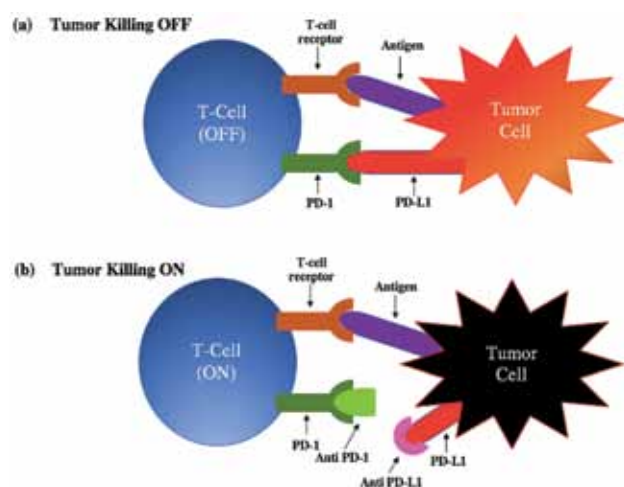


**Figure 1:** Schematic of immune checkpoint mechanisms. (a) Tumors can express PD-L1, which interacts with PD-1 receptors found on T cells, leading to suppression of the anti-tumor T cell response. (b) Inhibitors for PD-L1 and PD-1 prevent this interaction, unleashing the T cell anti-tumor response.

## 2. MATERIALS AND METHODS

### 2.1 Cloning and expression of CyPet-Ext.PDL1 and YPet-Ext.PD1

The recombinant vectors pET28(b)-CyPet-Ext.PDL1 and pET28(b)-YPet-Ext.PD1 (external domain: extracellular domain plus transmembrane) were cloned into competent *Escherichia coli* DH5 $\alpha$  bacterial cells and respectively plated on LB agar plates supplemented with 50  $\mu$ g/ml kanamycin. The recombinant vectors were then transferred to *Escherichia coli* BL21(DE3) for expression of recombinant protein. Transformed *E. coli* BL21(DE3) were plated on LB plates supplemented with 50  $\mu$ g/ml kanamycin to ensure transformation.<sup>9</sup> Single isolated clones of CyPet-Ext.PDL1 and YPet-Ext.PD1 were inoculated in 10 mL LB tubes and incubated overnight at 37°C with 220 rpm (revolutions per minute). A 1 L culture was then inoculated with 10 mL of the starting culture and allowed to grow to exponential phase approximately for 3 hours at 37°C and 220 rpm with shaking, Isopropyl  $\beta$ -D-1-thiogalactopyranoside (IPTG) in final concentration of 0.2 mM was added to induce, or enhance the expression of, the proteins. Aliquots were collected before and after addition of IPTG for SDS-PAGE analysis. The incubation parameters were lowered to 20°C and 150 rpm with shaking and the culture allowed to express for 16 hours.

### 2.2 Purification of recombinant CyPet-Ext.PDL1 and YPet-Ext.PD1

CyPet-Ext.PDL1 and YPet-Ext.PD1 cells were harvested by centrifugation for 15 minutes and pellets were washed and resuspended in lysis buffer then subjected to sonication for 15 minutes for each sample. After sonication cell lysates were centrifuged at 35,000 g for 30 minutes, and both supernatants and pellets were examined by using 10% SDS-PAGE to verify the location and expression of CyPet-Ext.PDL1 and YPet-Ext.PD1. The pellets were resuspended in denaturing buffer, incubated at 37°C for 15 minutes, and further incubated overnight at 4°C and shaken to completely dissolve the pellets and denature the proteins within the solution. Finally, the denatured proteins were centrifuged and the supernatants, which held the dissolved and denatured proteins, were purified by affinity chromatography on nickel nitrilotriacetic acid (Ni-NTA) gel matrix. Columns of Ni-NTA nitrocellulose resin were washed and equilibrated with denaturing buffer

first, then cleared cell lysates (containing CyPet-Ext.PDL1 and YPet-Ext.PD1) were loaded onto separate columns to be rinsed with wash buffer. The fractions were collected and examined with SDS-PAGE to evaluate the purity. The supernatants were also subjected to a Bradford assay to examine the concentrations of the CyPet-Ext.PDL1 and YPet-Ext.PD1 proteins.

### 2.3 Refolding of recombinant CyPet-Ext.PDL1 and YPet-Ext.PD1

The proteins must be dialyzed against dialysis buffer in order to remove the imidazole concentration and wash buffer. Protein filtrates for CyPet-Ext.PDL1 and YPet-Ext.PD1 were obtained via column chromatography and

Buffer/Solution	Reagents	pH
Lysis Buffer	20 M Tris-HCL, 0.5 M NaCl, 5 mM Imidazole	7.4
Wash Buffer and Denaturing Buffer	6M Guanidine-HCL, 0.5M Arg, 50 mM Tris-HCL, 0.5 M NaCl, 10 mM DTT	8.0
Dialysis Buffer A	4 M Guanidine-HCL, 0.5 M Arg, 50 mM Tris-HCL, 50 mM NaCl, 1 M DTT	8.0
Dialysis Buffer B	2 M Guanidine-HCL, 0.5 M Arg, 50 mM Tris-HCL, 50 mM NaCl, 1 M DTT	8.0
Dialysis Buffer C	1 M Guanidine-HCL, 0.5 M Arg, 50 mM Tris-HCL, 50 mM NaCl, 1 M DTT	8.0
Dialysis Buffer D	0.5 M Guanidine-HCL, 0.5 M Arg, 50 mM Tris-HCL, 50 mM NaCl, 1 M DTT	8.0
Dialysis Buffer E	0.25 M Guanidine-HCL, 0.5 M Arg, 50 mM Tris-HCL, 50 mM NaCl, 1 M DTT	8.0
Dialysis Buffer F	0.5 M Arg, 50 mM Tris-HCL, 50 mM NaCl, 1 M DTT	8.0
Dialysis Buffer G	0.25 M Arg, 50 mM Tris-HCL, 50 mM NaCl, 1 M DTT	8.0
Dialysis Buffer H	0.5 M Arg, 50 mM Tris-HCL, 50 mM NaCl, 1 M DTT	8.0

**Table 1**  
List of different buffers used in expression and purification of protein

poured into economical biotech dialysis membranes and dialyzed against dialysis buffer containing decreasing concentrations of Guanidine-HCL (6M, 4M, 2M, 1M, 0.5M, 0.25M and 0M – dialysis buffers A through H) for 16 hours in each concentration (*see Table 1*).

### 2.4 qFRET assay

30  $\mu\text{L}$  of purified and refolded recombinant CyPet-Ext.PDL1 and YPet-Ext.PD1, both at 0.5  $\mu\text{M}$ , were transferred into a 384-well plate (Greiner black) and the fluorescence emission spectrum of each well was measured with a fluorescence multi-well plate reader (Molecular Devices, FlexstationII<sup>384</sup>). Recombinant CyPet-Ext.PDL1 and YPet-Ext.PD1 proteins were also mixed together and diluted with phosphate buffered saline (PBS) to a total volume of 30  $\mu\text{L}$ . The final concentration of CyPet-Ext.PDL1 was fixed to 0.5  $\mu\text{M}$  and the final concentration of YPet-Ext.PD1 varied from 0 to 6  $\mu\text{M}$ . The mixtures were also transferred into a 384-well plate and the fluorescence emission spectrum of each well was measured. Two excitation wavelengths were used: 414 nm to excite CyPet, and 475 nm to excite YPet (*see Figure 2*).

The concentration of YPet-Ext.PD1 in both free and bound forms can be converted to functions of  $E_{\text{FRET}}$  (sensitized emission from YPet-Ext.PD1), since it is proportional to the amount of YPet-Ext.PD1 bound to CyPet-Ext.PDL1. Song et al. derived an equation for  $E_{\text{FRET}}$ , where  $FL_{\text{DD}}$  is the excited fluorescence signal of donor,  $FL_{\text{AA}}$  is the excited fluorescence signal of acceptor, 'x' is the CyPet ratio factor, and 'y' is the YPet ratio factor (*see Equation 1*).<sup>13</sup>

$$E_{\text{FRET}} = (E_{\text{total}}) - (x * FL_{\text{dd}}) - (y * FL_{\text{AA}}) \quad (1)$$

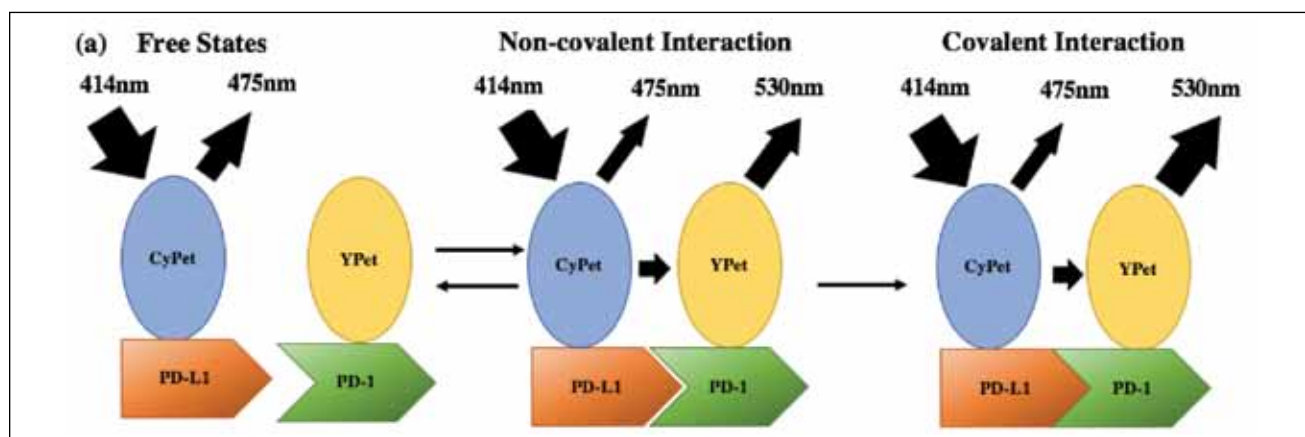


**Figure 2:** Design and detection of high sensitive FRET-based detection for PD-L1/PD-1 protein interactions.



Protein	Volume Cultured	IPTG Concentration	Fluorescent Protein Yield	% Purity based on SDS-PAGE
CyPet-Ext.PDL1	2 L	0.2 mM	0.2 $\mu$ M	~80
YPet-Ext.PD1	1 L	0.2 mM	8 $\mu$ M	~87

Table 2

### 3. Results

#### 3.1 Expression, purification, and dialysis of recombinant proteins

Induced, un-induced, cell pellet, cell lysate, and purified & refolded (from inclusion bodies) samples for both YPet-Ext.PD1 and CyPet-Ext.PDL1 were examined by using 10% SDS-PAGE to detect the active expression products (see Figure 3a). The induced and un-induced samples for both YPet-Ext.PD1 and CyPet-Ext.PDL1 (Figure 3a – lanes 1, 2, 6 & 7) show thicker bands than the others, denoting some protein expression, with the induced sample displaying higher expression.

Cell pellet and cell lysate samples for both YPet-Ext.PD1 and CyPet-Ext.PDL1 (Figure 3a – lanes 3, 4, 8 & 9) were also examined. The cell pellet samples for both proteins displayed darker and thicker bands than their cell lysate correlates. The concentration results via Bradford assay of the supernatants (lysates) and pellets for CyPet-Ext.PDL1 and YPet-Ext.PD1 showed high concentration of Ext.

PDL1 protein but low concentration of Ext.PD1 protein (see Table 2). The purified, dialyzed, and refolded samples of YPet-Ext.PD1 and CyPet-Ext.PDL1, rescued from their cell pellets, were visualized in Figure 3a – lanes 5 & 10. These bands were lighter than the bands shown for their cell pellets (Figure 3a – lanes 3 & 8), correlating to the recovery and purification of the proteins of interest from pellets and cellular debris.

#### 3.2 qFRET confirmation

Measuring the fluorescence spectrum of both purified and refolded CyPet-Ext.PDL1 and YPet-Ext.PD1 proteins showed a maximum RFU (relative fluorescent unit) value for CyPet-Ext.PDL1 at approximately  $3.8 \times 10^5$  for its emission wavelength of 475 nm and a maximum RFU value for YPet-Ext.PD1 at approximately  $1.6 \times 10^7$  for its emission wavelength of 530 nm (Figure 3b). It was found that the CyPet fluorescent protein has a lower quantum yield than the YPet protein, thus emission at the same protein concentration was lower for CyPet-Ext.PDL1.<sup>4</sup> The  $E_{\text{MFRET}}$  versus concentration of YPet-Ext.PD1 plot shows an increase in  $E_{\text{MFRET}}$  as the concentration of the acceptor (YPet-Ext.PD1) increases (see Figure 4).

## 4. DISCUSSION

### 4.1 PD-L1/PD-1

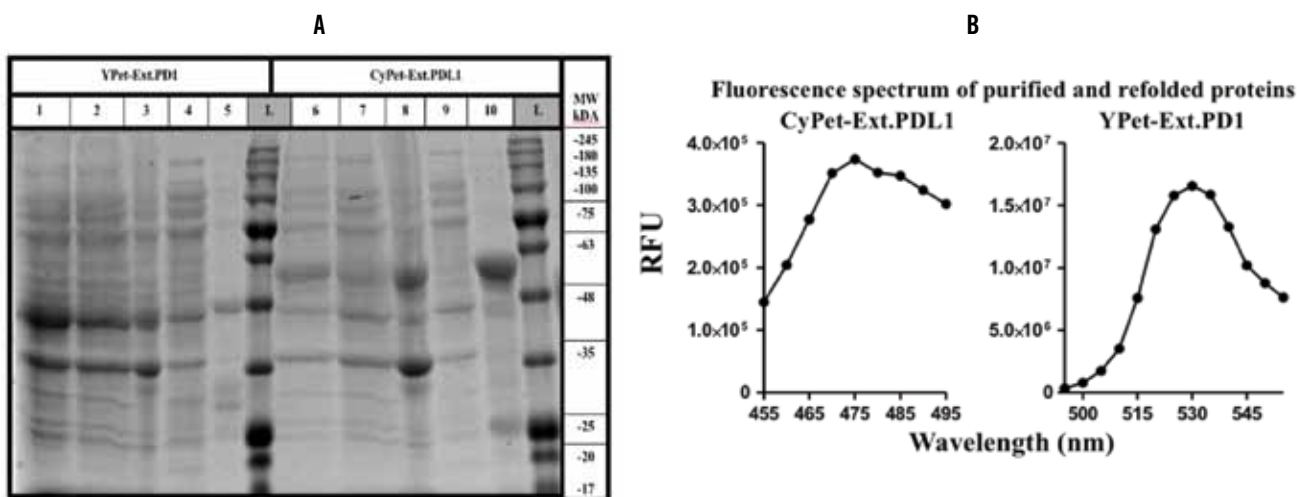


**Figure 3:** (a) SDS-PAGE gel, coomassie stain for determination of protein expression and validation of protein purification. 1-BL21(DE3) YPet-Ext.PD1 Induced expression, 2-BL21(DE3) YPet-Ext.PD1 Un-induced, 3-Cell Pellet, 4-Cell Lysate, 5-Purified and refolded from inclusion body YPet-Ext.PD1, 6-BL21(DE3) CyPet-Ext.PDL1 Induced expression, 7-BL21(DE3) CyPet-Ext.PDL1 Un-induced, 8-Cell Pellet, 9-Cell Lysate, 10-Purified and refolded from inclusion body CyPet-Ext.PDL1. MW of YPet-Ext.PD1 is 48 kDa and CyPet-Ext.PDL1 is 58 kDa. (b) The fluorescence spectrum was measured on FlexstationII384 of CyPet-Ext.PDL1 and YPet-Ext.PD1 both at 0.5  $\mu$ M, with excitation at 414 nm and 475 nm respectively. The CyPet fluorescent protein has a lower quantum yield than the YPet protein, thus emission at the same concentration is lower.

Expression of the induced and un-induced CyPet-Ext.PDL1 and YPet-Ext.PD1 proteins (**Figure 3a – lanes 1, 2, 6 & 7**) demonstrated that the pET28(b) vector functioned properly. It was observed that the samples of the cell pellets for both CyPet-Ext.PDL1 and YPet-Ext.PD1 held higher amounts of protein than in their cell lysates (**Figure 3a – lanes 3, 4, 8 & 9**), correlating to the understanding that PD-1 and PD-L1 are insoluble proteins that need to be rescued from cell pellets. **Figure 3a – lanes 5 & 10** confirmed the ability to recover, isolate, and purify these proteins out of the denaturing conditions. CyPet-Ext.PDL1 and YPet-Ext.PD1 proteins were able to remain solubilized once the denaturant (guanidine) had been removed from the dialysis buffers, and the addition of arginine to the buffers (**shown in Table 1**) helped the proteins stay in solution. It was observed in previous iterations that without arginine, the proteins of interest would go back to being insoluble after removal of the denaturant.<sup>14</sup>

#### 4.2 qFRET

The fluorescence spectrum of CyPet-Ext.PDL1 and YPet-Ext.PD1 shown in **Figure 3b** provided evidence of the presence of isolated fluorescent tagged proteins and confirmed that the CyPet fluorescent protein has a lower quantum yield than the YPet fluorescent protein. The  $E_{mFRET}$  plot in **Figure 4** showed that as the concentration of YPet-Ext.PD1 increased from 0  $\mu\text{M}$  to 1.0  $\mu\text{M}$ , and the CyPet-Ext.PDL1 concentration was held constant at 0.25  $\mu\text{M}$ , there was an increase in  $E_{mFRET}$  RFU. This provided evidence of acceptor (YPet-Ext.PD1) and donor (CyPet-

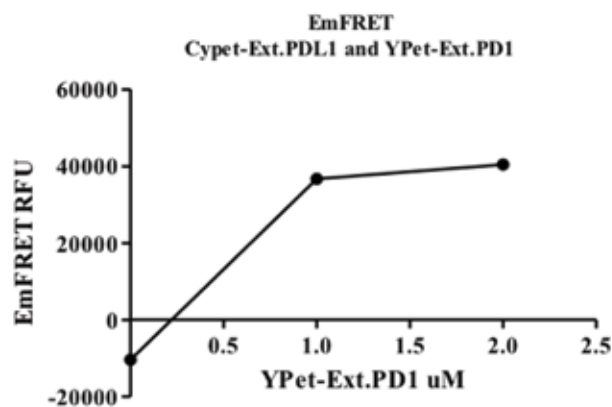


**Figure 4:** Plot of  $E_{mFRET}$  versus the acceptor YPet-Ext.PD1. The donor, CyPet-Ext.PDL1, concentration was held constant at 0.25  $\mu\text{M}$  and the concentration of YPet-Ext.PD1 was increased. The readings were taken on the FlexStationII384. Plot generated on GraphPad Prism.

Ext.PDL1) interaction. Furthermore, as YPet-Ext.PD1 concentration increased from 1.0  $\mu\text{M}$  to 2.0  $\mu\text{M}$ , a maximal FRET signal, or a plateau in the FRET signal, was noted. This implied that all of the CyPet-Ext.PDL1 and YPet-Ext.PD1 were paired and no additional FRET signal could be detected.

#### 5. Conclusion

PD-L1 has particular importance as a potential target for adaptive immunity and the protein-protein interaction of PD-L1 and PD-1 is a highly valued drug target for cancer immunotherapy. Past studies isolated the extracellular domain of PD-L1 for characterization of the structure. In this study, the insolubilized CyPet-Ext.PDL1 and YPet-Ext.PD1 proteins were put through a dialysis array to solubilize them. After completely removing the denaturant, protein precipitation was overcome by adding arginine, correlating to previous studies.<sup>14</sup> The initial yields of YPet-Ext.PD1 and CyPet-Ext.PDL1 (denatured within the cell lysate) were 22  $\mu\text{M}$  and 0.5  $\mu\text{M}$  respectively. The final yields were observed to be 8  $\mu\text{M}$  for purified YPet-Ext.PD1 and 0.2  $\mu\text{M}$  for purified CyPet-Ext.PDL1, showing that a large amount of protein was lost during the dialysis process. Additionally, a large difference between the inherent expression levels of PD-1 and PD-L1 was observed. The fluorescence spectrum measurement verified independent fluorescent tagged protein activity and the qFRET technique applied to the combination of YPet-Ext.PD1 and CyPet-Ext.PDL1 proteins reported their binding interaction.

Currently, methods to improve the initial yield of CyPet-Ext.PDL1 through codon optimization and or a SUMO tag to enhance expression levels are being investigated.<sup>3,10</sup> For future studies, a protein kinetic analysis of the  $K_d$  (dissociation constant) between PD-1 and PD-L1 can be performed. The results acquired in this experiment give insight into a novel technology, qFRET, that can be utilized to study the interaction between PD-1 and PD-L1. This technique is a platform for future research into high-throughput drug screening of small molecule inhibitors including antibodies, protein kinetic studies, and the utilization of FRET as a reporter for cell-surface protein interactions. Quantitative FRET technology holds a bright future for discovering immunotherapeutic agents with high efficacy and tolerability.

## ACKNOWLEDGMENTS

This work was supported by the Undergraduate Education Quarterly Minigrant from the University of California, Riverside. In addition, this study would not have been possible without the mentorship of Dr. Jiayu Liao and the support of graduate student Vipul Madahar.

## REFERENCES

- [1] Alsaab HO, Sau S, Alzhrani R, Tatiparti K, Bhise K, Kashaw SK, Iyer AK. PD-1 and PD-L1 checkpoint signaling inhibition for cancer immunotherapy: mechanism, combinations, and clinical outcome. *Frontiers in Pharmacology*. 2017;8:561. doi: 10.3389/fphar.2017.00561.
- [2] Bertucci F, Goncalves A. Immunotherapy in breast cancer: The emerging role of PD-1 and PD-L1. *Current Oncology Reports*. 2017;19(10):64. doi: 10.1007/s11912-017-0627-0.
- [3] Chen D, Texada DE. Low-usage codons and rare codons of escherichia coli. *Gene Therapy and Molecular Biology*. 2006;10:1-12.
- [4] Day RN, Davidson MW. The fluorescent protein palette: tools for cellular imaging. *Chemical Society Reviews*. 2009;38:2887-2921. doi: 10.1039/b901966a.
- [5] Global PD-1/PD-L1 inhibitors market report 2017 featuring Keytruda, Tecentriq, Imfinzi & Bavencio. *Cision PR Newswire*. 2018. Retrieved from <https://www.prnewswire.com/news-releases/global-pd-1pd-l1-inhibitors-market-report-2017-featuring-keytruda-tecentriq-imfinzi--bavencio-300581331.html>
- [6] Hino R, Kabashima K, Kato Y, Yagi H, Nakamura M, Honjo T, Okazaki T, Tokura Y. Tumor cell expression of programmed cell death-1 ligand 1 is a prognostic factor for malignant melanoma. *Cancer*. 2010;116(7):1757-1766. doi: 10.1002/cncr.24899.
- [7] Hussain SA. An introduction to fluorescence resonance energy transfer (FRET). *Tripura University*. 2009;1:1-4. doi: arXiv:0908.1815v1.
- [8] Janji B, Noman MZ, Viry E, Hasmim M, Messai Y, Berchem G, Chouaib FM, Chouaib S. Emerging role of hypoxia-induced autophagy in cancer immunotherapy. *Autophagy*. 2014;3:247-262. doi: 10.14800/ccm.213.
- [9] Kalim M, Chen J, Wang S, Lin C, Ullah S, Liang K, Ding Q, Chen S, Zhan J. Construction of high level prokaryotic expression and purification system of PD-L1 extracellular domain by using Escherichia coli host cell machinery. *Immunology Letters*. 2017;190:34-41. doi: 10.1016/j.imlet.2017.06.004.
- [10] Malakhov, MP, Mattern MR, Malakhova OA, Drinker M, Weeks SD, Butt TR. SUMO fusions and SUMO-specific protease for efficient expression and purification of proteins. *Journal of Structural and Functional Genomics*. 2004;5:75-86.
- [11] Meng X, Liu Y, Zhang J, Teng F, Xing L, Yu J. PD-1/PD-L1 checkpoint blockades in non-small cell lung cancer: new development and challenges. *Cancer Letters*. 2017;405:29-37. doi: <https://doi.org/10.1016/j.canlet.2017.06.033>.
- [12] Sekar RB, Periasamy A. Fluorescence resonance energy transfer (FRET) microscopy imaging of live cell protein localizations. *The Journal of Cell Biology*. 2013;160(5):629-633. doi: 10.1083/jcb.200210140.
- [13] Song Y, Madahar V, Liao J. Development of FRET assay into quantitative and high throughput screening technology platforms for protein-protein interactions. *Annals of Biomedical Engineering*. 2011;39(4):1224-1234. doi: 10.1007/s10439-010-0225-x.
- [14] Wang Y, van Oosterwijk N, Ali AM, Adawy A, Anindya AL, Dömling AS, Groves MR. A systematic protein refolding screen method using the DGR approach reveals that time and secondary TSA are essential variables. *Scientific Reports*. 2017;7(9355):1-10. doi:10.1038/s41598-017-09687-z.